

## **Climatic control on detrital sedimentation in the continental margin off Chennai, western Bay of Bengal– A 42 kyr record**

**Tyson Sebastian<sup>1,2</sup>, B. Nagender Nath<sup>1\*</sup>, Pavan Miriyala<sup>3</sup>, P. Linsy<sup>1, 2</sup>, Muralidhar Kocherla<sup>1</sup>**

<sup>1</sup>CSIR- National Institute of Oceanography, Dona Paula, Goa, India, 403004

<sup>2</sup>National Centre for Polar and Ocean Research, Goa, India, 403 804

<sup>3</sup>CSIR – National Geophysical Research Institute,  
Uppal Road, Hyderabad, India, 500007

\*Corresponding author email: nagendernath@yahoo.com

Dr. Tyson Sebastian - tysonsebastian@gmail.com

Dr. Pavan Miriyala - pavanmiriyala10@gmail.com

Dr. P. Linsy – linsymohan@gmail.com

Dr. Muralidhar Kocherla - kocherla@nio.org

### **Abstract**

While the peninsular Indian rivers deliver considerable loads of detrital sediments to the Bay of Bengal, changes in their depositional patterns with time are relatively less constrained compared to those deposited by Himalayan Rivers. Here, we present a 42 kyr record of detrital sedimentation, studied using whole-core logging, environmental magnetism, and major element geochemistry from the continental margin near Chennai, in the western Bay of Bengal. The variations of magnetic mineral properties and elemental concentrations of detrital sediments combined with the published oxygen isotope record, suggest monsoonal control on detrital input to the margin. Four major periods of changes in sedimentation are identified 1) the lower section of the core representing marine isotope stage (MIS) 3 (42 – 24 ka) shows varying detrital input, while magnetic minerals are affected by early diagenesis, 2) the period between 24 and 15 ka exhibits increased detrital input as a result of subaerial erosion in southern India during the last glacial sea-level lowstand, 3) the deglacial period from 15 to 10 ka is marked by decreased detrital input and increased productivity, and 4) the Holocene (10 – 2 ka) period experienced increased detrital input and chemical weathering in the source areas. Although the post-depositional alteration of magnetic minerals in MIS 3 limits the use of environmental magnetism, major elements and  $\delta^{18}\text{O}$  record the variations in paleomonsoon and detrital input during this period. The increased detrital input during 24 – 15 ka, despite the glacial conditions and intensified NE winter monsoon, indicates the increased subaerial erosion of exposed continental shelf during the sea-level lowstand owing to the proximity of the sampling site to the coast. The high magnetic susceptibility ( $\chi_{lf}$ ), chemical index of alteration (CIA), Al and Ti content beginning at ~10 ka marks the intensification of SW summer monsoon through the Holocene.

**Keywords:** Environmental magnetism, Geochemistry, Monsoonal precipitation, Sea-level change, Subaerial erosion, Chemical weathering.

## 1. Introduction

The Bay of Bengal (BoB) is a unique semi-enclosed basin in the northeastern Indian Ocean with a large freshwater influx and strong vertical stratification (Shetye et al., 1996). Although the seasonally reversing monsoonal circulation strongly influences the surface hydrography of both the BoB and the Arabian Sea, the BoB is less productive compared to the Arabian Sea owing to the strong stratification and weaker monsoon winds, which inhibit vertical mixing (Prasanna Kumar et al., 2002).

Sedimentary records from the river-fed continental margins such as the eastern continental margin of India can hold valuable information on the depositional processes, paleoclimate, tectonics, sea-level changes, and hydrodynamic conditions that control the detrital sedimentation to the coastal ocean. They document the complex sedimentary processes during the past periods with differing boundary conditions, such as the Last Glacial Maximum (LGM) when the sea-level was ~120 m lower than Present (Vaz, 2000). While the sediment records from the submarine fan environment and deep-sea settings in BoB are susceptible to turbiditic sedimentation and mixing from different sources (Babu et al., 2010; Kessarkar et al., 2005; Sangode et al., 2001), the continental margin sediments record the detrital sedimentation and freshwater fluxes from the peninsular Indian rivers.

The erosional and weathering history of Himalayan and Indo-Burman ranges are extensively studied across different timescales using sediments from the BoB and the Andaman Sea (e.g., Derry and France-Lanord, 1996; Colin et al., 1999; Nath et al., 2005; Rahaman et al., 2009; Tripathy et al., 2011; Lupker et al., 2013; Miriyala et al., 2017; Sebastian et al., 2019a, Ali et al., 2021; Bretschneider et al., 2021). Those studies report several events of increased erosion and weathering related to changes in the monsoon climate and orogeny in the Himalayas and Indo-Burman ranges. In contrast, the erosional and weathering history of peninsular India on the east coast is poorly constrained except for a few studies (e.g., Keshav and Achyuthan, 2015; Peketi et al., 2020), and thus, it is not known if the climate-induced weathering/erosion events of this area are coeval with those in Himalayan-Tibetan-Indo-Burman regions.

The southwestern BoB receives detrital sediments from the peninsular rivers such as Cauvery, Pennar, and Vaigai with their drainage basins comprising Precambrian gneisses and granulites (Selvaraj et al., 2004; Sebastian et al., 2019b). In areas such as these, precipitation (Indian monsoon in this case) and sea-level changes control the weathering and erosional processes. These rivers mainly flow through the southern states of India, and predominantly through Tamil Nadu, which receives major part of its annual rainfall during the northeast monsoon (NEM) season (from

October to December, e.g., Balachandran et al., 2006), which is also termed as winter monsoon. Thus, the detrital sedimentation history of the continental margin can provide information on the paleomonsoon strength in the source areas. Here, the detrital sedimentation history of the last 42 kyr of the continental margin near Chennai, is reconstructed using environmental magnetism and geochemical proxies. The data presented define distinct periods of climate-driven erosion, chemical weathering in the watersheds of southern India, and productivity changes in the western BoB, which are mainly linked to the changes in the Indian monsoon.

## **2. Materials and methods**

### **2.1. Sampling**

The sediment core (SSK 50 – GC 14A) analyzed in this study was collected from the continental margin off Chennai in the western Bay of Bengal (13° 29' 58" N, 80° 34' 30" E) from a water depth of 325 m, during the 50<sup>th</sup> cruise of RV Sindhu Sankalp in May 2013 (**Fig. 1**). The core is 2.82 m long and stored at 4°C. The core location falls within the present-day depths of the core oxygen minimum zone (OMZ) in the area.

### **2.2. Physical properties**

Physical properties of the core GC 14A were measured before subsampling by using a Multi-Sensor Core Logger (MSCL –X, Geotek, UK) at CSIR – National Institute of Oceanography, Goa, India. The whole core (the 2.82 m long core was split into three sections of 82 cm, 100 cm, and 100 cm lengths) was logged at room temperature. The bulk density of the sediment core [hereafter referred to as Gamma Ray Density (GRD)] was measured by passing gamma photons from a <sup>137</sup>Cs source through the sediment core and measuring its attenuation. GRD measurements were calibrated using a cylindrical rod of aluminium placed in a sealed core liner containing distilled water. Gamma counts of the aluminium rod obtained at different thicknesses, each for a 100 second time, were used to prepare the calibration curve (Best and Gunn, 1999).

Magnetic susceptibility was measured using a Bartington loop sensor (MS2C) of 150 mm internal diameter. A stable iron oxide calibration standard provided with the MSCL system, which has been tested and analyzed by the manufacturer, was used for calibrating the loop sensor. Following MSCL logging, the core was subsampled at 1 cm intervals, and samples were oven-dried below 50°C for further analyses.

### 2.3. Environmental magnetism

The environmental magnetic concentration, grain size and mineralogical parameters were measured on dried samples at CSIR – NIO, Goa. Magnetic susceptibility ( $\chi$ ) (both low frequency (0.47 kHz) and high frequency (4.7 kHz)) measurements were carried out using a Bartington MS2B sensor, while Anhyseretic remnant magnetization (ARM) was measured using a dual-speed spinner magnetometer (JR-6, AGICO, Brno, Czech Republic) after applying a 100 mT peak alternating field and a 0.05 mT constant bias field using a Molspin AF demagnetizer. Isothermal remnant magnetization (IRM) was imparted using a Molspin pulse magnetizer and saturation isothermal remnant magnetization (SIRM) was measured at a pulse-field of 1T (for more details of these analyses, refer to Sebastian et al., 2017).

### 2.4. Geochemistry

Major elements in the core were measured using Wavelength-Dispersive X-ray Fluorescence (XRF-WD; Axios, PANanalytical, The Netherlands) at CSIR - NIO, Goa. Decarbonated and salt-free (to represent lithogenic fraction) powdered samples (0.55 g) were mixed with Spectromelt® A12 (Merck) flux at 1180 °C in a furnace to make homogenous borate beads. Data quality was assessed using the marine sediment reference materials JMS-1, and JSO-1 (Geological Survey of Japan), and the accuracy of geochemical analyses was within  $\pm 4\%$  for JMS-1 and  $\pm 7\%$  for JSO-1.

The published chronology, oxygen isotope of planktonic foraminifera *Globigerinoides sacculifer*, organic carbon content (Sarathchandraprasad, 2019), carbonate Ca, Al, and Ti data from the same core (Sarathchandraprasad and Banakar, 2018) are used to support the primary data of this paper.

### 2.5. Chronology of the core

The chronology of the core established by Sarathchandraprasad and Banakar, (2018) estimated an age of 42.7 ka for the bottom of the core (282 cm) and 1.8 ka for the top. The radiocarbon dating was done on mixed planktonic foraminifera at NSF Arizona AMS Laboratory. The measured radiocarbon ages were corrected for a reservoir age of 331 years estimated for western BoB, north of Sri Lanka (Dutta et al., 2001), and were converted into calendar age using CalPal-7 calibration (Sarathchandraprasad, 2019). The radiocarbon ages along with lab reference numbers and calibrated ages are presented in **Table S1** (Sarathchandraprasad, 2019). The Bølling-Ållerød (14.7–12.7 ka) and Younger Dryas (YD) (12.7–11.7 ka) periods were identified from the oxygen isotope record of a mixed layer dwelling planktonic foraminifer *G. sacculifer* and were used as tie points to the chronology of a nearby well-dated sediment core (SK218/1, Govil and Naidu, 2011). The same

size fraction of foraminiferal tests (250-355 microns) was used in both studies. Additionally, a comparison of the mixed layer  $\delta^{18}\text{O}$  record (*G. sacculifer*) of GC 14A (this study) with other  $\delta^{18}\text{O}$  records from the region (Govil and Naidu, 2011; Raza et al., 2014, Kudrass et al., 2001, Joshi et al., 2014) and GISP2  $\delta^{18}\text{O}$  record (Stuiver and Grootes, 2000) reveals a good match during major climatic periods (**Fig. 2**) indicating the robustness of the chronology. The average sedimentation rate for the last 43 kyr was 6.87 cm/kyr.

### 3. Results

#### 3.1. Physical properties

The gamma-ray density (GRD) values of the sediment core GC 14A range between 1.44 and 1.86 g/cc with higher values during 15 – 10 ka (average 1.69 g/cc). The lowest values of GRD (average – 1.5 g/cc) are observed for the Holocene section. The volume-specific magnetic susceptibility obtained from the MSCL measurement of the core GC 14A ranges between 9 and  $62 \times 10^{-5}$  SI units (average –  $34.6 \times 10^{-5}$  SI units). Magnetic susceptibility is higher during mid to late Holocene (8 – 2 ka) and MIS 2 (24 – 15 ka) with a small decrease during the LGM (21 – 17 ka) and a rapid decrease during marine isotopic stage 3 (MIS 3).

#### 3.2. Environmental magnetism

The low and high frequency susceptibilities ( $\chi_{lf}$ ,  $\chi_{hf}$ ), Susceptibility of Anhysteretic Remanent Magnetization ( $\chi_{arm}$ ), and Saturated Isothermal Remanent Magnetization (SIRM) are proportional to the concentration of magnetic minerals present in the sediments (Thompson and Oldfield, 1986). High magnetic mineral concentrations are observed during the marine isotope stages (MIS) 1 and 2 except during 15 – 10 ka, where the values drop drastically (**Fig. 4**). Whole-core values of low frequency mass-specific magnetic susceptibility ( $\chi_{lf}$ ) range between 11 and  $99 \times 10^{-8}$   $\text{m}^3\text{kg}^{-1}$  with an average value of  $47.6 \times 10^{-8}$   $\text{m}^3\text{kg}^{-1}$ .  $\chi_{arm}$  and SIRM, vary between 0.08 and  $2.73 \times 10^{-5}$   $\text{m}^3\text{kg}^{-1}$  (average –  $1.49 \times 10^{-5}$   $\text{m}^3\text{kg}^{-1}$ ) and 190 -  $2807 \times 10^{-5}$   $\text{Am}^2\text{kg}^{-1}$  (average -  $1327 \times 10^{-5}$   $\text{Am}^2\text{kg}^{-1}$ ), respectively. The magnetic mineral concentration parameters  $\chi_{lf}$ ,  $\chi_{arm}$  and SIRM exhibited average values of  $24.1 \times 10^{-8}$   $\text{m}^3\text{kg}^{-1}$ ,  $0.55 \times 10^{-5}$   $\text{m}^3\text{kg}^{-1}$  and  $537 \times 10^{-5}$   $\text{Am}^2\text{kg}^{-1}$  respectively during MIS 3 compared to average values of  $65.6 \times 10^{-8}$   $\text{m}^3\text{kg}^{-1}$ ,  $2.2 \times 10^{-5}$   $\text{Am}^2\text{kg}^{-1}$  and  $1931 \times 10^{-5}$   $\text{Am}^2\text{kg}^{-1}$  during MIS 1 and 2. The ratios of  $\chi_{arm}/\chi_{lf}$ ,  $\chi_{arm}/\text{SIRM}$ , and  $\text{SIRM}/\chi_{lf}$  are indicative of magnetic mineral grain size (Oldfield, 1991; Thompson and Oldfield, 1986; Walden, 1999). Records of  $\chi_{arm}/\text{SIRM}$ ,  $\text{SIRM}/\chi_{lf}$  and  $\chi_{arm}/\chi_{lf}$ , in the present study reveal finer grain sizes during MIS 1 and 2, while a coarsening is observed in MIS 3 sediments. Grain size decreases with increasing values of  $\chi_{arm}/\text{SIRM}$  and  $\chi_{arm}/\chi_{lf}$ , whereas higher values of  $\text{SIRM}/\chi_{lf}$  imply a coarser magnetic grain size (Thompson and Oldfield, 1986).

Maximum values of  $\chi_{arm}/SIRM$  and  $\chi_{arm}/\chi_{lf}$  are observed between 15 – 10 ka indicating the finest magnetic grain size during this period. The magnetic mineralogical parameter S-ratio (an indicator of the relative proportions of ferromagnetic and canted antiferromagnetic minerals in the sample) and Hard IRM (HIRM, an indicator of the concentration of canted antiferromagnetic minerals such as hematite and goethite) suggest magnetite is the dominant magnetic mineral in MIS 1 and 2. The rapid decrease in the S-ratio in MIS 3 along with the magnetic mineral concentration denotes a decrease in the magnetite content. The consistent trend of HIRM profile during the MIS 3 indicates no change in the contribution from antiferromagnetic minerals despite the decrease in magnetite.

### 3.3. Geochemistry of the core

The concentration of refractory elements Al and Ti, indicative of terrigenous sedimentation and are unlikely to be affected by diagenesis, vary between 7.4 to 8.8 % and 0.55 to 0.78%, respectively. While high concentrations of Si are found in the sediments deposited between 15 and 10 ka, Al, and Ti concentrations were reduced during this period (**Fig. 5**). To assess the biogenic silica content in the samples, excess silica representing the biogenic silica, was calculated following the method described in Nath et al., (1989)

$$SiO_{2excess} = SiO_2 - 3.38 \times Al_2O_3 \quad (1)$$

Where 3.38 is the  $SiO_2/Al_2O_3$  ratio for the average deep-sea clay. The Chemical Index of Alteration (CIA) of the sediment defined as  $Al_2O_3/(Al_2O_3 + CaO^* + Na_2O + K_2O) \times 100$  (in molecular proportions of elemental oxides,  $CaO^*$  - CaO content in the silicate fraction of the sample) was calculated to assess the degree of weathering (Nesbitt and Young, 1982). The CIA values range between 69 and 79 with peak values during the Holocene. The organic carbon ( $C_{org}$ ) content in the core varies between 1.76 and 6.92 wt.% with higher content during 42 – 32 ka (average 3.56 wt.%) compared to the period between 32 and 2 ka (average 2.28 wt.%) (Sarithchandraprasad and Banakar, 2018) (**Fig. 6**). The minimum Ca concentration in the core (2.2%) is interpreted as a non-carbonate terrigenous component, as it is comparable with values of 2.3% found for Cauvery River sediment (Sarithchandraprasad and Banakar, 2018). The carbonate Ca content was calculated by subtracting the silicate Ca from the total Ca concentration, which varied between 1.9 and 18 wt.% (average 7.1 wt.%), with the highest content found during 15 – 10 ka (**Fig. 6**).

### 4. Discussion

The environmental magnetic parameters of continental margin sediments are primarily influenced by the detrital magnetic mineral content and thus are often used as a proxy to characterize the terrigenous sediment sources, temporal variations in continental erosion at source,

and the dispersal pathways of terrigenous sediments provided that the post-depositional alteration does not affect the magnetic signals (Thompson and Oldfield, 1986; Horng and Huh, 2011, Johnson et al., 2021, Sebastian et al., 2019b). Magnetic susceptibility data was effectively used to decipher the sources, distribution, and sediment dispersal pathways in the continental margins of India (Sebastian et al., 2019b). Susceptibility values were typically different for sediments derived from weathering of Deccan basalts from those derived from felsic sources. On the other hand, records of mineral magnetic grain size parameters ( $\chi_{arm}/SIRM$ ,  $SIRM/\chi_{lf}$ ,  $\chi_{arm}/\chi_{lf}$ ) from the Andaman Sea were used to identify periods of intensification in chemical weathering and switch to physical weathering, responding to the SW summer monsoon in source areas. (Sebastian et al., 2019a). To complement the environmental magnetism studies, geochemical proxies are used here to assess the changes in terrigenous and biogenous sedimentation in the depositional area. Major elements Ti and Al employed here are refractory in nature and not susceptible to secondary processes and thus are diagnostic of lithogenic input (e.g., Nath et.al., 1989) and provenance (e.g., Kurian et.al.,2013). Chemical index of alteration (CIA –Nesbitt and Young, 1982) and K to Al ratios have been used here to trace the silicate/chemical weathering in source areas (Nath et.al., 2000, Miriyala et.al., 2017). For deciphering changes in biogenic sedimentation, calcium carbonate, organic carbon and opal/biogenic silica (Nath, 2001 and references therein) are used. These environmental magnetic and geochemical studies supported by published oxygen isotope data of planktic foraminifera have revealed four major periods of depositional changes in detrital sedimentation for the last 42 kyrs in the western Bay of Bengal, viz., 1) the MIS 3 (42 – 24 ka) characterized by varying detrital input, fluctuations in bottom water oxygenation and post-depositional alteration of magnetic minerals, 2) the last glacial period from 24 to 15 ka with increased erosion and detrital input, 3) the deglaciation from 15 to 10 ka with reduced runoff facilitating increased biological productivity, and 4) the Holocene (10 – 2 ka) characterized by high detrital input and strong chemical weathering in source areas. These periods of depositional change are chronologically discussed below.

#### **4.1. Detrital sedimentation, post-depositional alteration of environmental magnetic parameters and paleoceanographic changes during MIS – 3 (42 – 24 ka)**

While the mixed layer dwelling planktonic foraminifer  $\delta^{18}O$  values are generally heavier for MIS 3 compared to the Holocene, suggesting generally a weaker summer monsoon, they are slightly lighter between 42 to 32 ka (except during Heinrich event H4), indicating a period of summer monsoon intensification (**Fig. 4**). This is almost consistent with the  $\delta^{18}O$  derived freshwater fluxes reported by Evans et al. (2015) from the central BoB, suggesting greater freshwater fluxes during 60 – 36 ka (**Fig. 5**). This is also consistent with other sediment records from BoB, which recorded

lighter  $\delta^{18}\text{O}$  values (Kudrass et al., 2001; Ota et al., 2019; Raza et al., 2014) and reduced sea-surface salinity (Kudrass et al., 2001) during 42 – 37 ka. An intensified SW monsoon during 42 – 37 ka is also reflected in our refractory element data with higher concentrations of Al and Ti (**Fig. 5**), suggesting an increased terrigenous input.

The diagenetic dissolution of iron oxides and their transformation into iron sulphides is a common phenomenon in reducing marine environments (Canfield and Berner, 1987; Karlin and Levi, 1983). The rapid decrease of magnetic mineral concentration parameters to near-zero values at 29 ka during MIS 3 is indicative of diagenetic alteration in of the magnetic minerals deposited during 42 – 29 ka. HIRM reflects the magnetic signal carried by the weakly magnetic, high coercivity antiferromagnetic minerals since it eliminates the contributions from ferrimagnetic minerals (Liu et al., 2007). S-ratio values close to unity (one) represent the dominance of low coercivity ferrimagnetic minerals, such as magnetite, while lower S-ratios reflect a higher concentration of antiferromagnetic minerals such as hematite (Liu et al., 2007; Thompson and Oldfield, 1986). The lower S-ratio during MIS 3 (average – 0.62) compared to the Holocene and MIS 2 (average 0.94) (**Fig. 4**), therefore suggests a loss of ferrimagnetic minerals such as magnetite through diagenesis. However, no significant change of the HIRM was observed during MIS 3 (average  $110.4 \pm 12.7$ ) compared to MIS 1 and 2 (average  $114.8 \pm 60.6$ ). The large decrease in S-ratio and the nearly constant HIRM during MIS 3 together suggest that diagenetic dissolution of magnetic minerals was confined to the ferrimagnetic fraction of the core (Bloemendal et al., 1993). During the post-depositional redox-mediated iron reduction in sediments, hematite is reported to be more stable than magnetite by many workers (e.g., Liu et al., 2004; Rey et al., 2005; Rowan et al., 2009). Diagenetic reactions are primarily due to the microbial processes involved during the decomposition of organic matter (e.g., Karlin et al., 1987, Roberts, 2015). The low oxygen condition (present-day bottom water oxygen concentration 0.18 mL/L) and high sedimentary organic carbon content (average 2.6%) at the core site favor the development of reductive diagenetic processes, but the alteration of environmental magnetic parameters seem to be confined to the sediments of MIS 3 between 42 and 24 ka.

The sedimentary organic carbon ( $C_{\text{org}}$ ) content was higher during MIS 3 (average 3.1%) compared to MIS 1 and 2 (average 2.3%) (Sarithchandraprasad and Banakar, 2018). The  $\delta^{13}\text{C}_{\text{org}}$  values of the core vary between -17.3 ‰ and -19.8 ‰, which reveal mixed marine and terrestrial sources of organic matter to the site (Sarithchandraprasad, 2019). Distinctly high  $C_{\text{org}}$  values are observed during 42 – 40 ka, 38 – 36 ka, 34 – 32 ka, 30 – 28 ka, 24 – 23 ka, and 13 – 11 ka. Carbonate Ca values show peaks during 38 – 36 ka, 34 – 33 ka, 30 – 28 ka, 24 – 23 ka, and 13 – 11 ka (**Fig. 6**). The  $C_{\text{org}}$  maxima during 38 – 36 ka, 30 – 28 ka, and 24 – 23 ka roughly coincide with the



North Atlantic cold Heinrich events 4, 3, and 2 suggesting the possibility of increased productivity during Northern Hemisphere cold periods (**Fig. 6**). A recent study from the Western BoB recorded prominent peaks of mixed-layer eutrophic species (*Globigerina bulloides*, *Globigerina glutinata* and *Globigerina falconensis*), during 43–41 ka, 39.5–38.5 ka, 35–34 ka, 31.5–30 ka, and 24–23 ka, indicating increased productivity (Verma et al., 2022). These periods roughly coincide with our  $C_{org}$  data within chronological uncertainties (**Fig. 6**). At present, the strong salinity stratification in BoB inhibits the advection of nutrient-rich water into the euphotic zone limiting primary production (Prasanna Kumar et al., 2002). Previous studies have recorded weakened summer monsoon and increased NE winter monsoon circulations during cold Heinrich stadials (Deplazes et al., 2014, Zorzi et al., 2015). This could have led to an enhanced supply of nutrient-rich subsurface water to the euphotic zone, thereby increasing the carbonate productivity. This is further supported by high *Globigerinabulloides*/*Globigerinoidesruber* ratios (a proxy that records changes in the mixed-layer environment) during Heinrich stadials from a nearby record (Verma et al., 2022) suggesting less stratified surface water conditions (**Fig. 6**).

The excess silica values show an inverse trend with carbonate Ca record during the Heinrich events 1, 2, 3, and 4. While the carbonate Ca record shows an increase during the Heinrich stadials, the excess silica values document a decreasing trend. Sediment trap data has shown that siliceous production increases in the Bay of Bengal during summer monsoon (Unger et al., 2003; Stoll et al., 2007), while the carbonate production is controlled by the nitrate availability (Prasanna Kumar et al., 2002, 2010; Madhupratap et al., 2003). In the Bay of Bengal, the upper 30 m of the water column is depleted of nitrate, suggesting no significant river input of nitrate to the open ocean (Prasanna Kumar, 2002). In contrast, the silicate concentrations in the upper 30 m of central and western Bay of Bengal are comparatively high, suggesting a riverine source (Prasanna Kumar et al., 2010). Ota et al., (2019) indicated that an increase in precipitation increases the influx of freshwater and riverine Si and results in a silicate dominant condition as the surface stratification restricts nitrate influxes from upwelling. Therefore, the inverse trend in the carbonate Ca and excess silica in our record can be used to differentiate the strong SW monsoon periods of higher riverine input from cold stadials associated with strong NE monsoon winds driven increased vertical mixing.

#### **4.2. Increased detrital influx during sea-level lowstand (24 – 15 ka): Evidence for erosion in source areas in peninsular India**

The environmental magnetic mineral and detrital element concentrations show an increased terrigenous input to the GC 14A core site during 24 – 15 ka except during the LGM where the concentrations decrease (**Figs. 4 and 5**). The volume magnetic susceptibility from the logging data

shows a notable increase from 24 ka to 15 ka, indicating increased terrigenous input to the site (**Fig. 3**). In unconsolidated sediments, GRD is often used as an indicator of the variations in mean grain size (Kim et al., 2012). Coarse-grained sediments display higher densities due to their lower porosity and increased grain-to-grain contact (Weber et al., 1997). During 24 – 15 ka, higher GRD density values (1.59 g/cc) compared to the Holocene (1.49 g/cc) indicate slightly coarser sediments. This is supported by higher concentrations of detrital elements Si, Al and Ti found during this period compared to the MIS 3 (**Fig. 5**). While Al is relatively refractory during weathering process. K tends to be enriched under moderate degrees of chemical weathering. At extreme chemical weathering conditions, K is depleted as K-feldspars break down. Therefore, a low (high) K/Al ratio in sediments can be considered as an indicator of intense (reduced) chemical weathering (e.g., Clift et al., 2014, Miriyala et.al., 2017).

Prevalence of a weak SW monsoon in the BoB during MIS 2 has been reported (Duplessy, 1982; Colin et al., 1999; Herzsuh, 2006; Rashid et al., 2011). The heavier  $\delta^{18}\text{O}$  values of mixed layer dwelling planktonic foraminifer during MIS 2 compared to Holocene in this core also point to a weaker monsoon. However, a higher detrital influx is observed in our record during the glacial period, when the SW monsoon was weak. The increased detrital sedimentation could be due to the glacial sea-level fall and the increased subaerial erosion when the distance between the source area and the depositional site would have reduced (**Fig. 7**). The global mean sea-level was more than 100 m lower during this period compared to the present day (Waelbroeck et al., 2002). In the BoB, near Chennai, Vaz (2000) estimated the sea-level during the LGM and found it to be lowest at 120 m below the present-day MSL. Banerjee (1993) has interpreted the channel upon channel features and subsurface channels (and valleys), which he found in the glacial sections of shallow seismic profiles across parts of the Coromandel inner shelf as due to the sea-level fall. These channels lie directly in front of present-day rivers and have been attributed to the incision of channels on the shelf following sea-level regression (Banerjee, 1993). The lowered sea-level resulted in the exposure of large part of the continental shelf and the sampling site would have been closer to potential sediment sources. Present-day, the core site is approximately 30 km away from the coastline, whereas it would have been closer to the coastline during the lowstand (**Fig.7**) and thus must have witnessed increased terrestrial sedimentation. The increased detrital input during the sea-level lowstand is also evident from the high values of  $\chi_{\text{lf}}$  and Ti contents which corresponds to the phase of lowered sea-level in the global mean sea-level curve (Waelbroeck et al., 2002) (**Fig. 8**). The coarser magnetic grain size evidenced from the lower values of grain size parameters  $\chi_{\text{arm}}/\text{SIRM}$  and  $\chi_{\text{arm}}/\chi_{\text{lf}}$  and higher values of  $\text{SIRM}/\chi_{\text{lf}}$  along with low CIA and high K/Al values suggest that physical weathering and erosion

were dominant and responsible for the increased sedimentation during the sea-level lowstand (Colin et al., 1998; Kissel et al., 2003; Sebastian et al., 2019a). A sediment core from Krishna Godavari Basin (MD161-8) in western BoB also shows a similar increase in Al content during this period (Peketi et al., 2020) (Please see **Fig. 5** for comparison). Increased detrital sedimentation during the glacial sea-level lowstand has been reported from various ocean basins, including the BoB (Li et al., 2019) and the South China Sea (Boulay et al., 2007; Huang et al., 2011; Liu et al., 2005).

#### **4.3. Reduced detrital flux and an increased productivity during last deglaciation (15 – 10 ka)**

A distinct decrease in the concentration of magnetic minerals, Al and Ti and a lower CIA with an increase in the GRD and carbonate Ca content is observed between 15 – 10 ka, all indicating decreased terrigenous input and increased productivity (**Figs. 4, 5 and 6**). The higher GRD values represent the coarsening of grain size, possibly due to the enhanced biogenic carbonate content (Snoeckx and Rea, 1995). Magnetic grain size parameters  $\chi_{\text{arm}}/\text{SIRM}$  and  $\chi_{\text{arm}}/\chi_{\text{lf}}$  show high values, indicating a finer magnetic grain size. The values of magnetic ratios  $\chi_{\text{arm}}/\text{SIRM}$  and  $\chi_{\text{arm}}/\chi_{\text{lf}}$  record average values of  $175 \times 10^{-5} \text{ mA}^{-1}$  and  $54.5 \times 10^3$  during 12.6 – 10 ka compared to the whole core average of  $103 \times 10^{-5} \text{ mA}^{-1}$  and  $27.8 \times 10^3$ . These are closer to the ratios in sediments showing bacterial magnetism ( $\chi_{\text{arm}}/\text{SIRM} > 200 \times 10^{-5} \text{ mA}^{-1}$  and  $\chi_{\text{arm}}/\chi_{\text{lf}} > 40 \times 10^3$  Oldfield, 1991; Thompson and Oldfield, 1986; Walden, 1999) and thus suggests the possible presence of bacterial magnetite in this sediment section.

The detrital sedimentation proxies Al, Ti, and  $\chi_{\text{lf}}$  record a decrease in concentration, while Si, unlike other detrital elements, shows an increase during 15 – 10 ka. This increase would thus require an additional source for Si besides the lithogenic sources. Another dominant silica-bearing component in marine sediments is biogenic silica which comes from skeletal remains of siliceous microfossils (Calvert, 1975; Nath et al., 1989). The increased  $\text{SiO}_2$  values during the period of reduced detrital input thus likely reflect the contribution of biogenic silica. This interpretation is also consistent with the increased productivity during 15 – 10 ka evident in the peaks of carbonate Ca and  $\text{C}_{\text{org}}$  content (**Fig. 6**). The  $\delta^{13}\text{C}$  values of this core reported by Sarathchandraprasad (2019) also record more negative values (average -18.9‰) during 15 – 10 ka compared to the Holocene (-17.8‰) and MIS 3 (-18.3‰), suggesting an increased contribution from marine organic matter during 15 – 10 ka. The  $\text{SiO}_{2\text{excess}}$  values showed a drastic increase during 15 – 10 ka (**Fig. 6**), indicating an increased biogenic silica content. The high  $\text{SiO}_{2\text{excess}}$  content suggests the increased siliceous productivity during 15 – 10 ka in the western BoB (**Fig. 6**). A gradual and sustained displacement of fauna with calcareous skeletons by siliceous tests at about 15 ka in a Northern BoB sediment core was reported by Contreras-Rosales et al. (2016). Another sediment record from the

northwestern BoB (NGHP-01-19B) reported a substantial increase in biogenic silica concentration since 13 ka, extending through the Holocene (Phillips et al., 2014). The decrease in terrigenous input and the increase in biogenic productivity during the deglaciation are consistent with the reduced freshwater influx into the western BoB during this period (Evans et al., 2015) (**Fig. 5**). Heavier mixed layer  $\delta^{18}\text{O}$  (*G. sacculifer*) during 15 - 10 ka (**Fig. 4**) also suggests a weak SW monsoon. Decreased CIA values and simultaneously increased K/Al ratios (**Fig. 5**) indicate weaker chemical weathering due to reduced humidity. The 15 – 10 ka period, except for the B/A has also witnessed an increase in sea surface salinity (SSS) in the BoB (Govil and Naidu, 2011) and in the Andaman Sea (Gebregiorgis et al., 2016; Sijinkumar et al., 2016) due to reduced freshwater runoff. This might have led to a weaker salinity stratification allowing increased vertical mixing of nutrients, thereby enhancing biological productivity (see Prasanna Kumar et al., 2002).

#### **4.4. Detrital input and monsoon variations during the Holocene (10 – 2 ka)**

The magnetic mineral concentration parameters increase from the beginning of Holocene towards the top of the core. While  $\chi_{\text{lf}}$  and SIRM continuously increase from early Holocene,  $\chi_{\text{arm}}$  (sensitive to the presence of stable single domain ferrimagnetic grains of  $\sim 0.02\text{--}0.04\ \mu\text{m}$  diameter) exhibits a mid-Holocene maximum and a subsequent decrease (**Fig. 4**) (Thompson and Oldfield, 1986). The magnetic grain size parameters  $\chi_{\text{arm}}/\text{SIRM}$  and  $\chi_{\text{arm}}/\chi_{\text{lf}}$  indicate a coarsening trend of magnetic grain size through the Holocene (Oldfield, 1991). This is also supported by increased HIRM and decreased S-ratio values suggesting an increase in the concentration of antiferromagnetic minerals such as hematite and goethite. The high detrital input during the Holocene is also supported by an increased concentration of detrital elements Ti and Al (average Ti content of - 0.47% and Al - 6.1%, for the Holocene compared to lower average values of Ti - 0.27% and Al - 4.13% for the 15 – 10 ka interval) (**Fig. 5**). At the same time, the Holocene has higher CIA values (average – 77.4) and low K/Al ratios, indicating the intensification of chemical weathering in the source areas (**Fig. 5**).

The mixed layer oxygen isotope data show lighter values in the Holocene, indicating wetter conditions and increased SW monsoon except for the mid-Holocene, where slightly heavier values are recorded, suggesting a reduction in rainfall (**Fig. 4**). The increased SW monsoon during the early Holocene agrees with other BoB and Andaman Sea records of monsoon intensification (Rashid et al., 2007; Govil and Naidu, 2011; Sijinkumar et al., 2016; Sebastian et al., 2019a) and enormous sediment discharge from Himalayan rivers (Goodbred and Kuehl, 2000). The magnetic and elemental record of GC 14A suggests a SW monsoon intensification beginning at 11 ka. The mid-Holocene weakening of the summer monsoon in this record is consistent with the other Indian

monsoon records from north of our core location (Ponton et al., 2012; Cui et al., 2017). While the mid-Holocene weakening of SW summer monsoon is comparable, the continued intensification of the monsoon and chemical weathering from mid- to late-Holocene observed in our record contrasts with the aridification and accelerated erosion in central India shown in a sedimentary plant wax carbon isotope record offshore river Godavari (Ponton et al., 2012; Giosan et al., 2017) and the shift in organic carbon source from C3 to C4 plants under the continued weak monsoon phase in Godavari delta record (Cui et al., 2017). This north-south contrast between the mid-Holocene arid conditions reported from offshore Godavari river records (Giosan et al., 2017; Ponton et al., 2012) and humid conditions in southeastern India (as inferred in this study) might reflect the influence of the NE winter monsoon in our record. Our sediment core is located off the southern state of Tamil Nadu in southeast Peninsular India, which receives a major part of its annual rainfall during the northeast (NE) monsoon season (the three-month period from October to December, e.g., Balachandran et al., 2006). So, it is possible that while central India has contributed eroded sediments, southeastern India must have supplied chemically weathered sediments, both contributing to the sediment build-up of the continental margin. The  $\chi_{lf}$  and mixed layer  $\delta^{18}O$  record of GC 14A (our record) compare well with the  $\delta^{18}O$  records (Govil and Naidu, 2011; Raza et al., 2014) and sea surface salinity record (Kudrass et al., 2001) in the northern BoB (Fig. 7) and appears to be coherent with the insolation at 15°N (Berger and Loutre, 1991; **Fig. 9**). Variations in solar insolation resulting from Earth's orbit are considered to have controlled the Indian Monsoon and appear to have determined the frequency of ENSO warm and cold events further influencing the climate of India (Dimri et al., 2016 and references therein).

## 5. Conclusions

The environmental magnetic and geochemical records of a sediment core GC 14A from the continental margin off Chennai, southeastern India, tracks the climatic control over the detrital sedimentation to the western Bay of Bengal during the last 42 kyr. The results indicate four major periods of varying detrital sedimentation; 1) varying detrital input, fluctuations in bottom water oxygenation and post-depositional alteration of magnetic minerals during MIS 3 (42 – 24 ka), 2) increased erosion and detrital input during 24 – 15 ka, 3) reduced runoff during the deglacial from 15 to 10 ka that has facilitated increased biological productivity, and 4) increased detrital input and chemical weathering in source areas during the Holocene (10 – 2 ka). Oxygen isotopes and geochemical records indicate SW summer monsoon intensification during 42 – 32 ka except during the Heinrich stadials. The high detrital input during 24 – 15 ka despite the glacial conditions and decreased SW monsoon corresponds well with the sea-level fluctuations indicating the increased

subaerial erosion of the exposed continental shelf during the LGM sea-level lowstand. The decrease in terrigenous input and the increase in biogenic productivity during 15 – 10 ka agrees with the reduced freshwater influx into the BoB. The weathering indices CIA and K/Al and the oxygen isotope data suggest an increasing trend in chemical weathering during Holocene due to summer monsoon intensification. The new depositional data of the late Pleistocene presented here add to the limited knowledge of past weathering and erosion in southern India.

### **Acknowledgements**

Authors are thankful to the Director of CSIR - NIO, Goa for providing the ship time and analytical facilities. Our sincere thanks to Dr. Ed Hathorne (IFM-GEOMAR) for his painstaking effort in correcting our text which has substantially improved the manuscript's readability. Dr. Firoz Badesab is gratefully acknowledged for providing the environmental magnetic analytical facilities. We thank colleagues from Ship Cell, other NIO participants and the crew members of 50<sup>th</sup> cruise of RV Sindhu Sankalp for helping us collect the sediment core used in this study. TS is thankful to CSIR - Shyama Prasad Mukherjee Fellowship (SPMF) for providing the research fellowship. Thanks are due to two anonymous reviewers for their constructive comments and the very detailed and meticulous editorial comments and inputs by Prof. A.D. Singh. This work is a contribution to CSIR XII Plan project GEOSINKS (PSC0106). This is CSIR - NIO's contribution No.XXXX.

### **Author Statement**

TS and BNN designed the study. TS analyzed the samples, interpreted the results, and drafted the manuscript. BNN led the project and helped in the interpretation of the results and revision of manuscript. PM and LP collected the samples onboard and helped in geochemical analyses. MK helped in XRF analyses. All authors were involved in the discussion and refinement of the final manuscript.

## References

- Ali, S., Hathorne, E.C., Frank, M., (2021). Persistent provenance of South Asian monsoon-induced silicate weathering over the past 27 million years. *Paleoceanogr. Paleoclimatology* 36, e2020PA003909. <https://doi.org/10.1029/2020PA003909>
- Babu, C. P., Pattan, J. N., Dutta, K., Basavaiah, N., Prakash Babu, C., Pattan, J. N., Dutta, K., Basavaiah, N., Ravi Prasad, G. V., Ray, D. K., and Govil, P. (2010). Shift in detrital sedimentation in the eastern Bay of Bengal during the late Quaternary. *Journal of Earth System Science*, 119(3), 285–295. <https://doi.org/10.1007/s12040-010-0022-9>
- Balachandran, S., Asokan, R., and Sridharan, S. (2006). Global surface temperature in relation to northeast monsoon rainfall over Tamil Nadu. *Journal of Earth System Science*, 115(3), 349–362. <https://doi.org/10.1007/BF02702047>
- Banerjee, P. K. (1993). Imprints of late Quaternary climatic and sea-level changes on East and South Indian coast. *Geo-Marine Letters*, 13(1), 56–60. <https://doi.org/10.1007/BF01204393>
- Berger, A., and Loutre, M. F. (1991). Insolation values for the climate of the last 10 million years. *Quaternary Science Reviews*, 10(4), 297–317. [https://doi.org/10.1016/0277-3791\(91\)90033-Q](https://doi.org/10.1016/0277-3791(91)90033-Q)
- Best, A. I., and Gunn, D. E. (1999). Calibration of marine sediment core loggers for quantitative acoustic impedance studies belonging to Southampton Oceanography Centre. *Marine Geology*, 160, 137–146. [https://doi.org/10.1016/S0025-3227\(99\)00017-1](https://doi.org/10.1016/S0025-3227(99)00017-1)
- Bloemendal, J., King, J. W., Hunt, A., Demenocal, P. B., and Hayashida, A. (1993). Origin of the sedimentary magnetic record at Ocean Drilling Program Sites on the Owen Ridge, western Arabian Sea. *Journal of Geophysical Research*, 98(B3), 4199. <https://doi.org/10.1029/92JB02914>
- Boulay, S., Colin, C., Trentesaux, A., Clain, S., Liu, Z., and Lauer-Leredde, C. (2007). Sedimentary responses to the Pleistocene climatic variations recorded in the South China Sea. *Quaternary Research*, 68(1), 162–172. <https://doi.org/10.1016/j.yqres.2007.03.004>
- Bretschneider, L., Hathorne, E.C., Huang, H., Lübbers, J., Kochhann, K.G.D., Holbourn, A., Kuhnt, W., Thiede, R., Gebregiorgis, D., Giosan, L., Frank, M., (2021). Provenance and Weathering of Clays Delivered to the Bay of Bengal During the Middle Miocene: Linkages to Tectonics and Monsoonal Climate. *Paleoceanogr. Paleoclimatology* 36, e2020PA003917. <https://doi.org/10.1029/2020PA003917>
- Calvert, S. E. (1975). Deposition and Diagenesis of Silica in Marine Sediments. In *Pelagic Sediments: On Land and under the Sea* (pp. 273–299). Blackwell Publishing Ltd. <https://doi.org/10.1002/9781444304855.ch12>
- Canfield, D.E., Berner, R.A., (1987). Dissolution and pyritization of magnetite in anoxic marine sediments. *Geochim. Cosmochim. Acta* 51, 645–659. [https://doi.org/10.1016/0016-7037\(87\)90076-7](https://doi.org/10.1016/0016-7037(87)90076-7)
- Clift, P. D., Wan, S., and Blusztajn, J. (2014). Reconstructing chemical weathering, physical erosion and monsoon intensity since 25Ma in the northern South China Sea: A review of competing proxies. *Earth-Science Reviews* 130, 86–102. <https://doi.org/10.1016/j.earscirev.2014.01.002>

- Colin, C., Kissel, C. L., Blamart, D., and Turpin, L. (1998). Magnetic properties of sediments in the Bay of Bengal and the Andaman Sea: impact of rapid North Atlantic Ocean climatic events on the strength of the Indian monsoon. *Earth and Planetary Science Letters*, 160, 623–635. [https://doi.org/10.1016/S0012-821X\(98\)00116-2](https://doi.org/10.1016/S0012-821X(98)00116-2)
- Colin, C., Turpin, L., Bertaux, J., Desprairies, A., and Kissel, C. (1999). Erosional history of the Himalayan and Burman ranges during the last two glacial–interglacial cycles. *Earth and Planetary Science Letters*, 171(4), 647–660. [https://doi.org/10.1016/S0012-821X\(98\)00116-2](https://doi.org/10.1016/S0012-821X(98)00116-2)
- Contreras-Rosales, L. A., Schefuß, E., Meyer, V., Palamenghi, L., Lückge, A., and Jennerjahn, T. C. (2016). Origin and fate of sedimentary organic matter in the northern Bay of Bengal during the last 18 ka. *Global and Planetary Change*, 146, 53–66. <https://doi.org/10.1016/J.GLOPLACHA.2016.09.008>
- Cui, M., Wang, Z., Nageswara Rao, K., Sangode, S. J., Saito, Y., Chen, T., Kulkarni, Y. R., Naga Kumar, K. C. V, and Demudu, G. (2017). A mid- to late-Holocene record of vegetation decline and erosion triggered by monsoon weakening and human adaptations in the south-east Indian Peninsula. *The Holocene*, 27(12), 1976–1987. <https://doi.org/10.1177/0959683617715694>
- Derry, L. A., and France-Lanord, C. (1996). Neogene Himalayan weathering history and river  $^{87}\text{Sr}/^{86}\text{Sr}$ : impact on the marine Sr record. *Earth and Planetary Science Letters*, 142(1–2), 59–74. [https://doi.org/10.1016/0012-821X\(96\)00091-X](https://doi.org/10.1016/0012-821X(96)00091-X)
- Deplazes, G., Lückge, A., Stuut, J.-B.W., Pätzold, J., Kuhlmann, H., Husson, D., Fant, M., Haug, G.H., (2014). Weakening and strengthening of the Indian monsoon during Heinrich events and Dansgaard-Oeschger oscillations. *Paleoceanography* 29, 99–114. <https://doi.org/10.1002/2013PA002509>
- Dimri, A. P., Yasunari, T., Kotlia, B. S., Mohanty, U. C., and Sikka, D. R. (2016). Indian winter monsoon: Present and past. *Earth-Science Reviews* 163, 297–322. <https://doi.org/10.1016/j.earscirev.2016.10.008>
- Duplessy, J. C. (1982). Glacial to interglacial contrasts in the northern Indian Ocean. *Nature*, 295(5849), 494–498. <https://doi.org/10.1038/295494a0>
- Dutta, K., Bhushan, R., Somayajulu, B.L.K., (2001).  $\Delta R$  correction values for the northern Indian Ocean. *Radiocarbon* 43, 483–488. <https://doi.org/10.1017/S0033822200038376>
- Evans, D., Bhatia, R., Stoll, H., and ME Uller, W. (2015). LA-ICPMS Ba/Ca analyses of planktic foraminifera from the Bay of Bengal: Implications for late Pleistocene orbital control on monsoon freshwater flux. *Geochemistry, Geophysics, Geosystems*, 16, 2598–2618. <https://doi.org/10.1002/2015GC005822>
- Gebregiorgis, D., Hathorne, E. C., Sijinkumar, A. V., Nath, B. N., Nürnberg, D., and Frank, M. (2016). South Asian summer monsoon variability during the last ~54 kas inferred from surface water salinity and river runoff proxies. *Quaternary Science Reviews*, 138, 6–15. <https://doi.org/10.1016/j.quascirev.2016.02.012>



- Giosan, L., Ponton, C., Usman, M., Blusztajn, J., Fuller, D. Q., Galy, V., Haghypour, N., Johnson, J. E., McIntyre, C., Wacker, L., and Eglinton, T. I. (2017). Massive erosion in monsoonal central India linked to late Holocene land cover degradation. *Earth Surface Dynamics*, 5(4), 781–789. <https://doi.org/10.5194/esurf-5-781-2017>
- Goodbred, S. L., and Kuehl, S. A. (2000). Enormous Ganges-Brahmaputra sediment discharge during strengthened early Holocene monsoon. *Geology*, 28(12), 1083. [https://doi.org/10.1130/0091-7613\(2000\)28<1083:EGSDDS>2.0.CO;2](https://doi.org/10.1130/0091-7613(2000)28<1083:EGSDDS>2.0.CO;2)
- Govil, P., and Naidu, P. D. (2011). Variations of Indian monsoon precipitation during the last 32 ka reflected in the surface hydrography of the western Bay of Bengal. *Quaternary Science Reviews*, 30, 3871–3879. <https://doi.org/10.1016/j.quascirev.2011.10.004>
- Hemming, S. R. (2004), Heinrich events: Massive late Pleistocene detritus layers of the North Atlantic and their global climate imprint, *Rev. Geophys.*, 42, RG1005, <https://doi.org/10.1029/2003RG000128>.
- Herzschuh, U. (2006). Palaeo-moisture evolution in monsoonal Central Asia during the last 50,000 years. *Quaternary Science Reviews*, 25, 163–178. <https://doi.org/10.1016/j.quascirev.2005.02.006>
- Horng, C. S., and C. A. Huh (2011), Magnetic properties as tracers for source-to-sink dispersal of sediments: A case study in the Taiwan Strait, *Earth Planet. Sci. Lett.*, 309, 141–152, doi:10.1016/j.epsl.2011.07.002
- Huang, E., Tian, J., and Steinke, S. (2011). Millennial-scale dynamics of the winter cold tongue in the southern South China Sea over the past 26ka and the East Asian winter monsoon. *Quaternary Research*, 75(1), 196–204. <https://doi.org/10.1016/j.yqres.2010.08.014>
- Johnson, J. E., Phillips, S. C., Clyde, W. C., Giosan, L., & Torres, M. E. (2021). Isolating detrital and diagenetic signals in magnetic susceptibility records from methane-bearing marine sediments. *Geochemistry, Geophysics, Geosystems*, 22, e2021GC009867. <https://doi.org/10.1029/2021GC009867>
- Joshi, R.K., Mazumdar, A., Peketi, A., Ramamurty, P.B., Naik, B.G., Kocherla, M., Carvalho, M.A., Mahalakshmi, P., Dewangan, P., Ramana, M.V., (2014). Gas hydrate destabilization and methane release events in the Krishna-Godavari basin, Bay of Bengal. *Mar. Petrol. Geol.* 58, 476–489. <https://doi.org/10.1016/j.marpetgeo.2014.08.013>
- Karlin, R., and Levi, S. (1983). Diagenesis of magnetic minerals in Recent hemipelagic sediments. *Nature*, 303(5915), 327–330. <https://doi.org/10.1038/303327a0>
- Karlin, R., Lyle, M., & Heath, G. R. (1987). Authigenic magnetite formation in suboxic marine sediments. *Nature*, 326(6112), 490–493. <https://doi.org/10.1038/326490a0>
- Keshav, N., and Achyuthan, H. (2015). Late Holocene continental shelf sediments, off Cuddalore, East coast, Bay of Bengal, India: Geochemical implications for source-area weathering and provenance. *Quaternary International*, 371, 209–218. <https://doi.org/10.1016/j.quaint.2015.03.002>

- Kessarkar, P. M., Rao, V. P., Ahmad, S. M., Patil, S. K., Anil Kumar, A., Anil Babu, G., Chakraborty, S., and SoundarRajan, R. (2005). Changing sedimentary environment during the Late Quaternary: Sedimentological and isotopic evidence from the distal Bengal Fan. *Deep Sea Research Part I: Oceanographic Research Papers*, 52(9), 1591–1615. <https://doi.org/10.1016/J.DSR.2005.01.009>
- Kim, G.Y., Bahk, J.J., Yoo, D.G., Ryu, B.J., (2012). Physical property interpretation using log data from the Ulleung basin sediments, East Sea of Korea. *Mar. Georesources Geotechnol.* 30, 195–209. <https://doi.org/10.1080/1064119X.2011.602387>
- Kissel, C., Laj, C., Clemens, S., and Solheid, P. (2003). Magnetic signature of environmental changes in the last 1.2 Myr at ODP Site 1146, South China Sea. *Marine Geology*, 201(1–3), 119–132. [https://doi.org/10.1016/S0025-3227\(03\)00212-3](https://doi.org/10.1016/S0025-3227(03)00212-3)
- Kudrass, H. R. R., Hofmann, A., Doose, H., Emeis, K., and Erlenkeuser, H. (2001). Modulation and amplification of climatic changes in the Northern Hemisphere by the Indian summer monsoon during the past 80 k.y. *Geology*, 29(1), 63. [https://doi.org/10.1130/0091-7613\(2001\)029<0063:MAAOCC>2.0.CO;2](https://doi.org/10.1130/0091-7613(2001)029<0063:MAAOCC>2.0.CO;2)
- Kurian, S., Nath, B.N., Kumar, N.C., Nair, K.K.C., 2013. Geochemical and isotopic signatures of surficial sediments from the western continental shelf of India: inferring provenance, weathering, and the nature of organic matter. *J. Sediment. Res.* 83, 427–442. <https://doi.org/10.2110/jsr.2013.36>
- Li, J., Liu, S., Shi, X., Zhang, H., Fang, X., Cao, P., Yang, G., Xue, X., Khokiattiwong, S., and Kornkanitnan, N. (2019). Sedimentary responses to the sea-level and Indian summer monsoon changes in the central Bay of Bengal since 40 ka. *Marine Geology*, 415, 105947. <https://doi.org/10.1016/j.margeo.2019.05.006>
- Liu, J., Zhu, R., Roberts, A.P., Li, S., Chang, J.-H., (2004). High-resolution analysis of early diagenetic effects on magnetic minerals in post-middle-Holocene continental shelf sediments from the Korea Strait. *J. Geophys. Res.* 109, B03103. <https://doi.org/10.1029/2003JB002813>
- Liu, Z., Colin, C., Trentesaux, A., Siani, G., Frank, N., Blamart, D., and Farid, S. (2005). Late Quaternary climatic control on erosion and weathering in the eastern Tibetan Plateau and the Mekong Basin. *Quaternary Research*, 63(3), 316–328. <https://doi.org/10.1016/j.yqres.2005.02.005>
- Liu, Q., Roberts, A.P., Torrent, J., Horng, C.-S., Larrasoana, J.C., (2007). What do the HIRM and S -ratio really measure in environmental magnetism? *Geochemistry, Geophys. Geosystems* 8, n/a-n/a. <https://doi.org/10.1029/2007GC001717>
- Lupker, M., France-Lanord, C., Galy, V., Lavé, J., and Kudrass, H. (2013). Increasing chemical weathering in the Himalayan system since the Last Glacial Maximum. *Earth and Planetary Science Letters*, 365, 243–252. <https://doi.org/10.1016/J.EPSL.2013.01.038>
- Madhupratap, M., Gauns, M., Ramaiah, N., Prasanna Kumar, S., Muraleedharan, P., de Sousa, S., Sardessai, S., Muraleedharan, U., (2003). Biogeochemistry of the Bay of Bengal: physical, chemical and primary productivity characteristics of the central and western Bay of Bengal during summer monsoon 2001. *Deep Sea Res. Part II Top. Stud. Oceanogr.* 50, 881–896. [https://doi.org/10.1016/S0967-0645\(02\)00611-2](https://doi.org/10.1016/S0967-0645(02)00611-2)

- Miriyala, P., Sukumaran, N. P. P., Nath, B. N. N., Ramamurthy, P. B. B., Sijinkumar, A. V. V., Vijayagopal, B., Ramaswamy, V., and Sebastian, T. (2017). Increased chemical weathering during the deglacial to mid-Holocene summer monsoon intensification. *Scientific Reports*, 7, 44310. <https://doi.org/10.1038/srep44310>
- Nath, B. N., Rao, V. P., and Becker, K. P. (1989). Geochemical evidence of terrigenous influence in deep-sea sediments up to 8° S in the Central Indian Basin. *Marine Geology*, 87(2–4), 301–313. [https://doi.org/10.1016/0025-3227\(89\)90067-4](https://doi.org/10.1016/0025-3227(89)90067-4)
- Nath, B.N., Kunzendorf, H., Pluger, W.L., (2000). Influence of provenancer weathering, and sedimentary processes on the elemental ratios of the fine-grained fraction of the bedload sediments from the Vembanad Lake and the adjoining continental shelf, southwest coast of India. *Journal of Sedimentary Petrology* 70,1081–1094. <https://doi.org/10.1306/100899701081>
- Nath, B. N. (2001). Geochemistry of sediments. In R. Sen Gupta & E. Desa (Eds.), *The Indian Ocean: A perspective* (Vol. 2, pp. 645–690). New Delhi: Oxford & IBH
- Nath, B. N., Gupta, S. M., Mislankar, P. G., Rao, B. R., Parthiban, G., Roelandts, I., and Patil, S. K. (2005). Evidence of Himalayan erosional event at ~0.5 Ma from a sediment core from the equatorial Indian Ocean in the vicinity of ODP Leg 116 sites. *Deep-Sea Research Part II: Topical Studies in Oceanography*, 52(14–15), 2061–2077. <https://doi.org/10.1016/j.dsr2.2005.05.011>
- Nesbitt, H. W., and Young, G. M. (1982). Early Proterozoic climates and plate motions inferred from major element chemistry of lutites. *Nature*, 299(5885), 715–717. <https://doi.org/10.1038/299715a0>
- Oldfield, F. (1991). Environmental magnetism - A personal perspective. *Quaternary Science Reviews*, 10(1), 73–85. [https://doi.org/10.1016/0277-3791\(91\)90031-O](https://doi.org/10.1016/0277-3791(91)90031-O)
- Ota, Y., Kawahata, H., Kuroda, J., Yamaguchi, A., Suzuki, A., Araoka, D., et al. (2019). Indian monsoonal variations during the past 80 kyr recorded in NGHP-02 Hole 19B, western Bay of Bengal: Implications from chemical and mineral properties. *Geochemistry, Geophysics, Geosystems*, 20, 148–165. <https://doi.org/10.1029/2018GC007772>
- Peketi, A., Mazumdar, A., Pillutla, S. P. K., Rai, V. K., Sawant, B., Chaitanya, A. V. S., and Krishna, R. (2020). Monsoon rainfall and contrasting source rocks influenced sediment composition of peninsular basins along the east coast of India (western Bay of Bengal). *Marine and Petroleum Geology*, 118, 104433. <https://doi.org/10.1016/j.marpetgeo.2020.104433>
- Phillips, S. C., Johnson, J. E., Giosan, L., and Rose, K. (2014). Monsoon-influenced variation in productivity and lithogenic sediment flux since 110 ka in the offshore Mahanadi Basin, northern Bay of Bengal. *Marine and Petroleum Geology*, 58, 502–525. <https://doi.org/10.1016/J.MARPETGEO.2014.05.007>
- Ponton, C., Giosan, L., Eglinton, T. I., Fuller, D. Q., Johnson, J. E., Kumar, P., and Collett, T. S. (2012). Holocene aridification of India. *Geophysical Research Letters*, 39(3), 1–6. <https://doi.org/10.1029/2011GL050722>

- Prasanna Kumar, S., Muraleedharan, P. M., Prasad, T. G., Gauns, M., Ramaiah, N., de Souza, S. N., Sardesai, S., and Madhupratap, M. (2002). Why is the Bay of Bengal less productive during summer monsoon compared to the Arabian Sea? *Geophysical Research Letters*, 29(24), 88-1-88-4. <https://doi.org/10.1029/2002GL016013>
- Prasanna Kumar, S., Nuncio, M., Narvekar, J., Ramaiah, N., Sardesai, S., Gauns, M., Fernandes, V., Paul, J.T., Jyothibabu, R., Jayaraj, K.A., (2010). Seasonal cycle of physical forcing and biological response in the Bay of Bengal. *Indian J. Mar. Sci.* 39 (3), 388–405.
- Rahaman, W., Singh, S. K., Sinha, R., and Tandon, S. K. (2009). Climate control on erosion distribution over the Himalaya during the past ~100 ka. *Geology*, 37(6), 559–562. <https://doi.org/10.1130/G25425A.1>
- Rashid, H., Flower, B. P., Poore, R. Z., and Quinn, T. M. (2007). A ~25ka Indian Ocean monsoon variability record from the Andaman Sea. *Quaternary Science Reviews*, 26(19), 2586–2597. <https://doi.org/10.1016/j.quascirev.2007.07.002>
- Rashid, H., England, E., Thompson, L., and Polyak, L. (2011). Late Glacial to Holocene Indian Summer Monsoon Variability Based upon Sediment Records Taken from the Bay of Bengal. *Terr. Atmos. Ocean. Sci.*, 22331917(10). <https://doi.org/10.3319/TAO>
- Raza, T., Ahmad, S. M., Sahoo, M., Banerjee, B., Bal, I., Dash, S., Suseela, G., and Mukherjee, I. (2014). Hydrographic changes in the southern Bay of Bengal during the last ~65,000 y inferred from carbon and oxygen isotopes of foraminiferal fossil shells. *Quaternary International*, 333, 77–85. <https://doi.org/10.1016/J.QUAINT.2014.02.010>
- Rey, D., Mohamed, K. J., Bernabeu, A., Rubio, B., and Vilas, F. (2005). Early diagenesis of magnetic minerals in marine transitional environments: geochemical signatures of hydrodynamic forcing. *Marine Geology*, 215(3–4), 215–236. <https://doi.org/10.1016/j.margeo.2004.12.001>
- Roberts, A. P. (2015). Magnetic mineral diagenesis. *Earth-Science Reviews*, 151, 1–47. <https://doi.org/10.1016/j.earscirev.2015.09.010>
- Rowan, C. J., Roberts, A. P., and Broadbent, T. (2009). Reductive diagenesis, magnetite dissolution, greigite growth and paleomagnetic smoothing in marine sediments: A new view. *Earth and Planetary Science Letters*, 277(1–2), 223–235. <https://doi.org/10.1016/j.epsl.2008.10.016>
- Sangode, S. J., Suresh, N., and Bagati, T. N. (2001). Godavari source in the Bengal fan sediments: Results from magnetic susceptibility dispersal pattern. *Current Science*, 80(5), 660–664.
- Sarithchandraprasad, T. (2019). Past oxygen minimum zone in the Bay of Bengal reconstruction from sedimentary particulate manganese: Implications to productivity variability. Goa University. <http://irgu.unigoa.ac.in/drs/handle/unigoa/5204?show=full>
- Sarithchandraprasad, T., and Banakar, V. K. (2018). Last 42 ky sediment chemistry of oxygen deficient coastal region of the Bay of Bengal: implications for terrigenous input and monsoon variability. *Current Science*, 114 (9), 1940-1946

- Sebastian, T., Nath, B. N., Venkateshwarlu, M., Miriyala, P., Prakash, A., Linsy, P., Kocherla, M., Yazing, A. K., and Sijinkumar, A. V. (2019a). Impact of the Indian Summer Monsoon variability on the source area weathering in the Indo-Burman ranges during the last 21 ka – A sediment record from the Andaman Sea. *Palaeogeography, Palaeoclimatology, Palaeoecology*, *516*, 22–34. <https://doi.org/10.1016/J.PALAEO.2018.11.035>
- Sebastian, T., Nath, B. N., Ramaswamy, V., Mascarenhas-Pereira, M. B. L., Yazing, A. K., Apurva, P. R., Linsy, P., Kocherla, M., Miriyala, P., and Rao, B. R. (2019b). Distribution and dispersal of surface sediments on the continental margins of India. *Marine and Petroleum Geology*, *110*, 122–137. <https://doi.org/10.1016/j.marpetgeo.2019.07.017>
- Sebastian, T., Nath, B. N., Naik, S., Borole, D. V., Pierre, S., and Yazing, A. K. (2017). Offshore sediments record the history of onshore iron ore mining in Goa State, India. *Marine Pollution Bulletin*, *114*(2), 805–815. <https://doi.org/10.1016/j.marpolbul.2016.10.075>
- Selvaraj, K., Ram Mohan, V., and Szefer, P. (2004). Evaluation of metal contamination in coastal sediments of the Bay of Bengal, India: geochemical and statistical approaches. *Marine Pollution Bulletin*, *49*(3), 174–185. <https://doi.org/10.1016/j.marpolbul.2004.02.006>
- Shetye, S. R., Gouveia, A. D., Shankar, D., Shenoi, S. S. C., Vinayachandran, P. N., Sundar, D., Michael, G. S., and Nampoothiri, G. (1996). Hydrography and circulation in the western Bay of Bengal during the northeast monsoon. *Journal of Geophysical Research: Oceans*, *101*(C6), 14011–14025. <https://doi.org/10.1029/95JC03307>
- Sijinkumar, A. V., Nagender Nath, B., and Clemens, S. (2016). North Atlantic climatic changes reflected in the Late Quaternary foraminiferal abundance record of the Andaman Sea, northeastern Indian Ocean. *Palaeogeography, Palaeoclimatology, Palaeoecology*, *446*, 11–18. <https://doi.org/10.1016/J.PALAEO.2016.01.009>
- Snoeckx, H., and Rea, D. K. (1995). CaCO<sub>3</sub> content and bulk density of leg 138 site-survey piston cores 1. *Scientific Results*, *138*. <https://doi.org/10.2973/odp.proc.sr.138.155.1995>
- Stoll, H.M., Arevalos, A., Burke, A., Ziveri, P., Mortyn, G., Shimizu, N., Unger, D., (2007). Seasonal cycles in biogenic production and export in Northern Bay of Bengal sediment traps. *Deep Sea Res. Part II Top. Stud. Oceanogr.* *54*, 558–580. <https://doi.org/10.1016/J.DSR2.2007.01.002>
- Stuiver, M., Grootes, P.M., (2000). GISP2 Oxygen isotope ratios. *Quat. Res.* *53*, 277–284. <https://doi.org/10.1006/qres.2000.2127>.
- Thompson, R., and Oldfield, F. (1986). *Environmental Magnetism*. Springer Netherlands. <https://doi.org/10.1007/978-94-011-8036-8>
- Tripathy, G. R., Singh, S. K., Bhushan, R., and Ramaswamy, V. (2011). Sr-Nd isotope composition of the Bay of Bengal Sediments: Impact of climate on erosion in the Himalaya. *Geochemical Journal*, *45*, 1–25. <https://doi.org/10.2343/geochemj.1.0112>
- Unger, D., Ittekkot, V., Schäfer, P., Tiemann, J., Reschke, S., (2003). Seasonality and interannual variability of particle fluxes to the deep Bay of Bengal: influence of riverine input and oceanographic processes. *Deep Sea Res. Part II Top. Stud. Oceanogr.* *50*, 897–923. [https://doi.org/10.1016/S0967-0645\(02\)00612-4](https://doi.org/10.1016/S0967-0645(02)00612-4)

- Vaz, G. G. (2000). Age of relict coral reef from the continental shelf off Karaikal, Bay of Bengal: Evidence of Last Glacial Maximum. *Current Science* 79, 228–230. <https://doi.org/10.2307/24103454>
- Verma, K., Singh, A.D., Singh, P., Singh, H., Satpathy, R.K., Uddandam, P.R., Naidu, P.D., (2022). Monsoon-related changes in surface hydrography and productivity in the Bay of Bengal over the last 45 kyr B.P. *Palaeogeogr. Palaeoclimatol. Palaeoecol.* 589, 110844. <https://doi.org/10.1016/J.PALAEO.2022.110844>
- Waelbroeck, C., Labeyrie, L., Michel, E., Duplessy, J.C., McManus, J.F., Lambeck, K., Balbon, E., Labracherie, M., (2002). Sea-level and deep water temperature changes derived from benthic foraminifera isotopic records. *Quat. Sci. Rev.* 21, 295–305. [https://doi.org/10.1016/S0277-3791\(01\)00101-9](https://doi.org/10.1016/S0277-3791(01)00101-9)
- Walden, J. (1999). Remanence measurements. In J. Walden, F. Oldfield, and J. Smith (Eds.), *Environmental magnetism: a practical guide* (Technical, pp. 63–87.). Quaternary Research Association, London.
- Weber, M.E., Niessen, F., Kuhn, G., Wiedicke, M., (1997). Calibration and application of marine sedimentary physical properties using a multi-sensor core logger. *Mar. Geol.* 136, 151–172. [https://doi.org/10.1016/S0025-3227\(96\)00071-0](https://doi.org/10.1016/S0025-3227(96)00071-0)
- Zorzi, C., Sanchez Goñi, M.F., Anupama, K., Prasad, S., Hanquiez, V., Johnson, J., Giosan, L., (2015). Indian monsoon variations during three contrasting climatic periods: The Holocene, Heinrich Stadial 2 and the last interglacial-glacial transition. *Quat. Sci. Rev.* 125, 50–60. <https://doi.org/10.1016/J.QUASCIREV.2015.06.009>

## Figure Captions

**Fig.1:** Map showing location of the sediment core GC 14A (Red). Core locations of other records (white) discussed in the text are also shown (SK 218-1 - Govil and Naidu, 2011; VM 29-19 - Rashid et al., 2011; RC12-343 - Duplessy, 1982; 126KL - Kudrass et al., 2001). Bathymetric data from <https://maps.ngdc.noaa.gov/viewers/wcs-client>.

**Fig. 2:** Oxygen isotope record of mixed layer dwelling planktonic foraminifer *Globigerinoides. sacculifer* of GC 14A (Sarathchandraprasad and Banakar 2018) along with  $\delta^{18}\text{O}$  records from the nearby areas in Bay of Bengal (Govil and Naidu, 2011; Raza et al., 2014, Kudrass et al., 2001, Joshi et al., 2014). The Greenland Ice Sheet Project 2 (GISP2)  $\delta^{18}\text{O}$  record is also plotted for comparison (Stuiver and Grootes, 2000). The dashed lines indicate the correlation between the different  $\delta^{18}\text{O}$  records.

**Fig.3:** Down-core variations of physical properties gamma ray density, volume magnetic susceptibility, and fractional porosity of the sediment core GC 14A. The core was scanned with the Multi Sensor Core Logger (MSCL) and the dotted lines mark the limits of core sections.

**Fig. 4:** Down-core variation of environmental magnetic mineral parameters in core GC 14A indicating the concentration, grain size and mineralogy of the magnetic minerals. Major climatic events Younger Dryas (YD), Heinrich events 1 – 4 (H1 – H4), and Last Glacial Maximum (LGM) are also shown. For the Heinrich events, the ages given in Hemming, (2004) are used. The zone affected by magnetic mineral diagenesis (42 – 29 ka) [evidenced by the rapid loss of  $\chi_{\text{lf}}$ ,  $\chi_{\text{arm}}$ , and SIRM concentration] and the zone retaining detrital signals (29 – 2 ka) are marked in the figure. The oxygen isotope data of the core is from Sarathchandraprasad and Banakar (2018).

**Fig. 5:** Down-core variation of detrital element concentrations Al, Ti and Si along with the geochemical ratios K/Al and Chemical Index of Alteration (CIA) of GC 14A. Al and Ti data are from Sarathchandraprasad and Banakar (2018). The freshwater influx data derived from the oxygen isotope values (Evans et al., 2015) for the BoB is also shown in the graph. Records of Al, K/Al and CIA (Peketi et al., 2020) from the Krishna Godavari Basin, western BoB are shown with dotted lines.

**Fig. 6:** Down-core distribution of excess silica (indicating biogenic silica), carbonate Ca and  $C_{\text{org}}$  in the core GC 14A indicating periods of increased surface productivity. Carbonate Ca is taken from Sarathchandraprasad and Banakar (2018), while  $C_{\text{org}}$  data are from Sarathchandraprasad (2019). A 3-point moving average has been used in smoothening the  $C_{\text{org}}$  data. Also plotted are the mixed-layer eutrophic species abundance data (MLES: *G. bulloides*, *G. glutinata* and *G. falconensis*), indicating mixed layer nutrient condition; and *G. bulloides*/*G. ruber* abundance ratio indicating surface stratification from a nearby record of core SK 218/1 off Krishna – Godavari basin (Verma et al., 2022). The freshwater flux data is from Evans et al. (2015). The sea surface salinity data is adopted from Govil and Naidu (2011).

**Fig. 7:** Schematic diagram showing the sea-level during a) present-day; and b) LGM. The lowered sea-level and the exposed continental shelf are marked. The bathymetry data are from <https://maps.ngdc.noaa.gov/viewers/wcs-client>.

**Fig. 8:** Graph showing the variation of detrital sedimentation proxies  $\chi_{\text{lf}}$  and Ti along with the global mean sea-level curve (Waelbroeck et al., 2002). The shaded region marks the glacial sea-level lowstand, which resulted in increased sedimentation due to the sub-aerial erosion of exposed shelf.

**Fig. 9:**  $\chi_{\text{LF}}$  and mixed layer planktic foraminifera (*G. sacculifer*)  $\delta^{18}\text{O}$  record of GC 14A along with nearby  $\delta^{18}\text{O}$  records (Govil and Naidu, 2011; Raza et al., 2014), sea surface salinity record (Kudrass et al., 2001) and the insolation at 15°N (Berger and Loutre, 1991).

## Supplementary Table captions

**Table S1:** Radiocarbon ages for the dated sections of GC 14A along with lab reference codes (NSF Arizona AMS Laboratory) and calibrated age as given in Sarathchandraprasad (2019). The measured radiocarbon ages were corrected for a reservoir age of 331 years estimated for western BoB, north of Sri Lanka (Dutta et al., 2001), and converted into calendar age using CalPal-7 calibration.



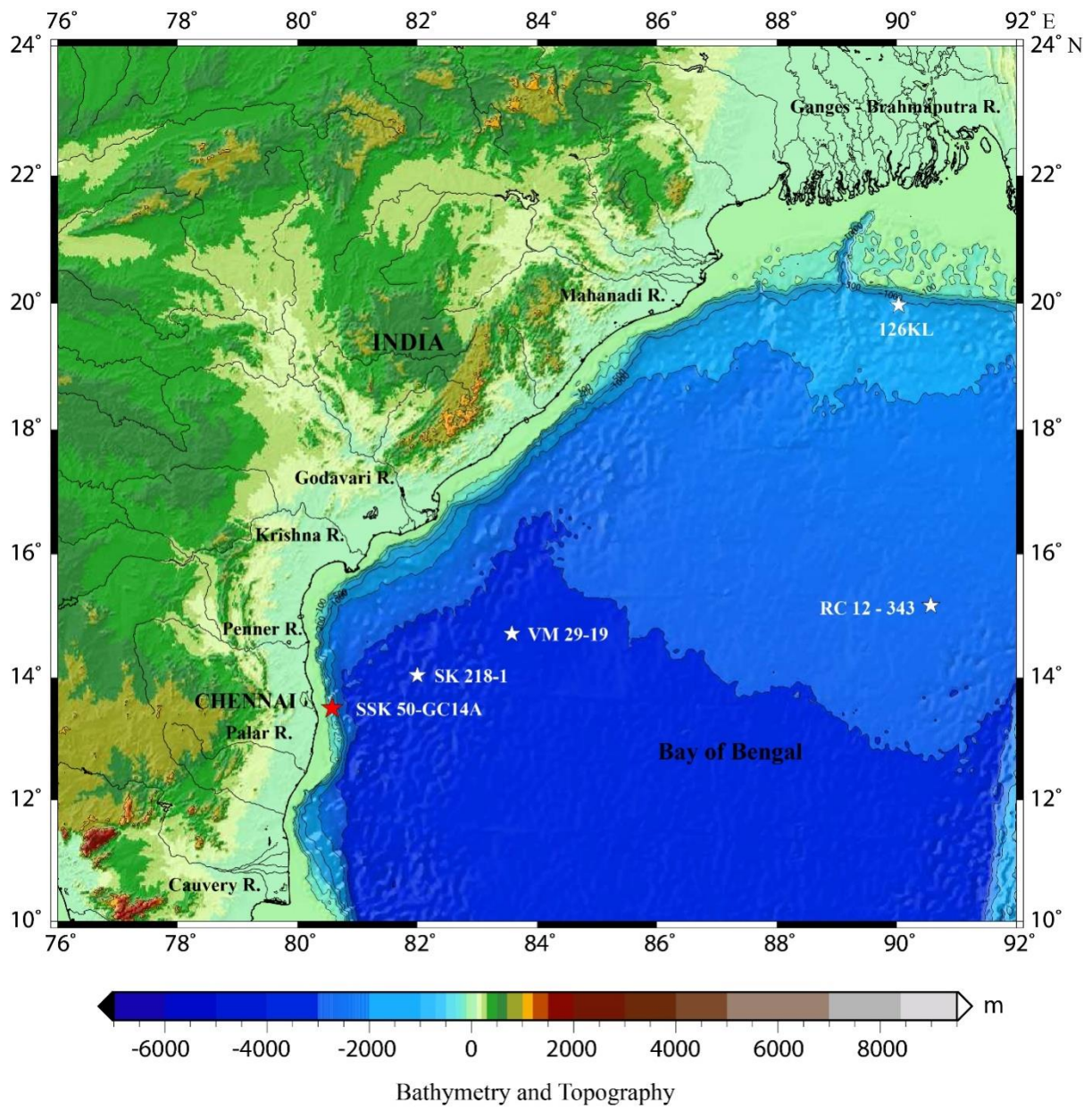


Figure 1



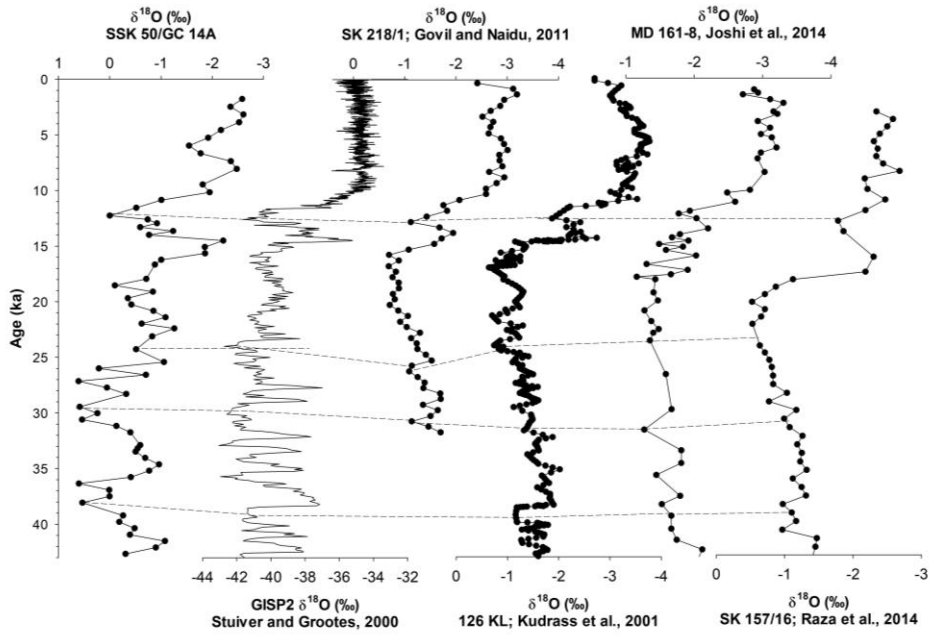


Fig. 2

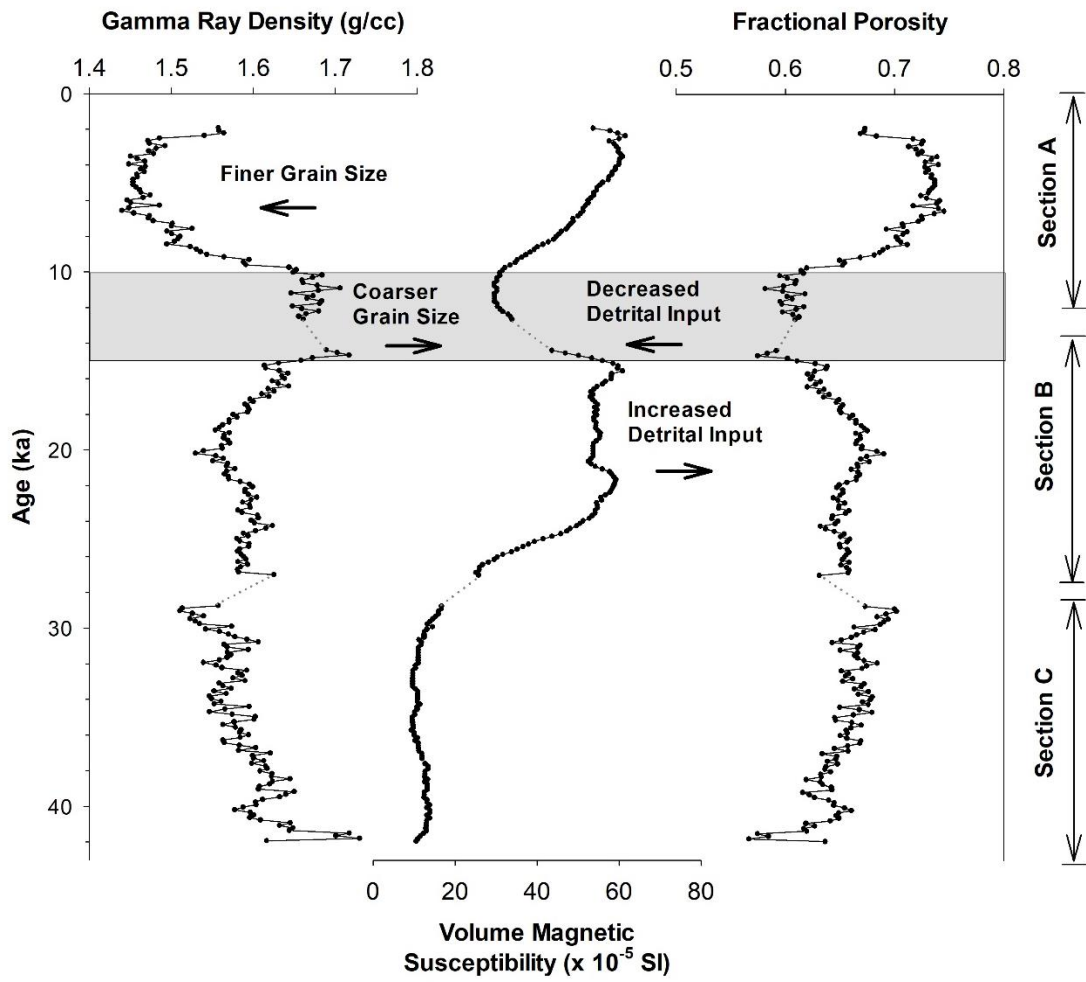


Figure 3

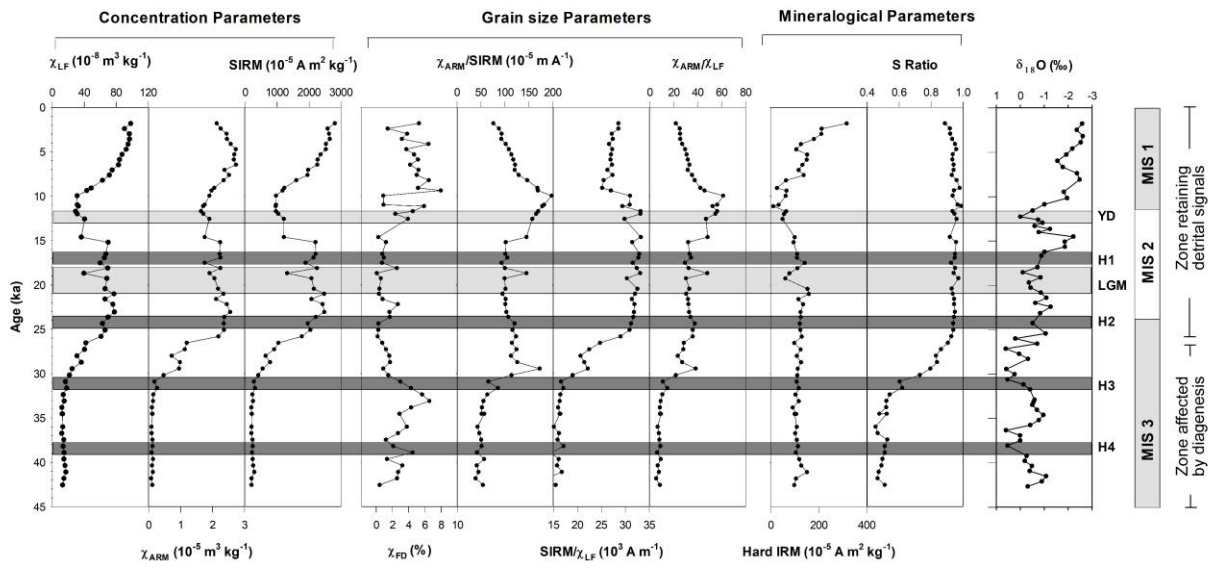


Figure 4

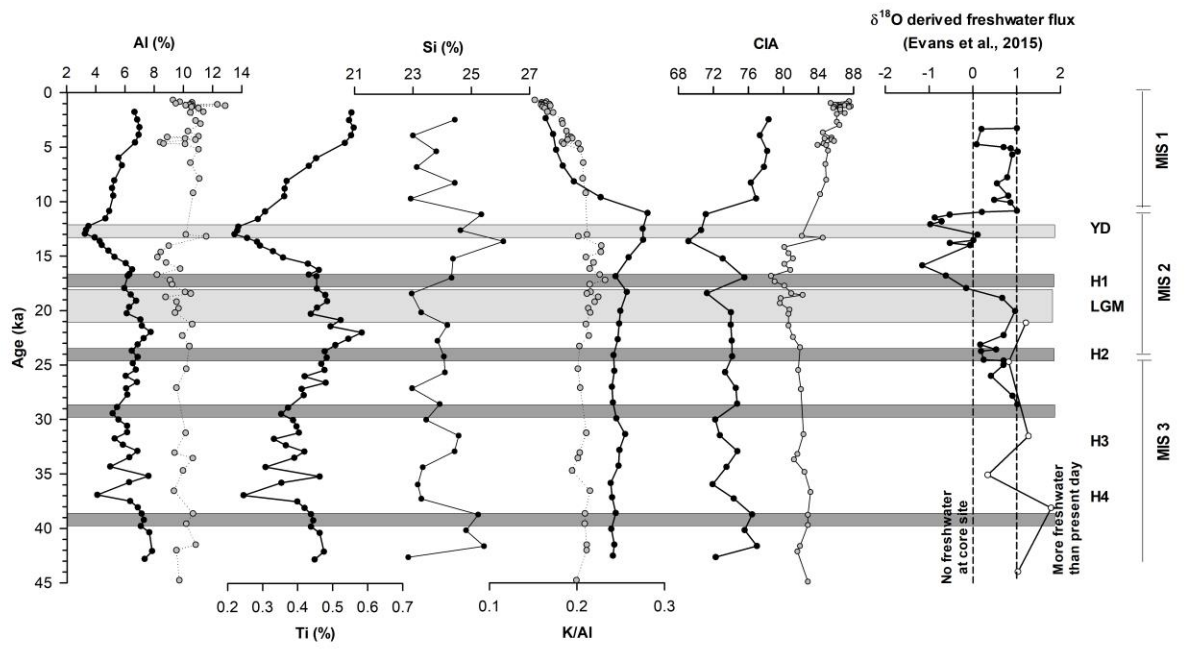


Figure 5

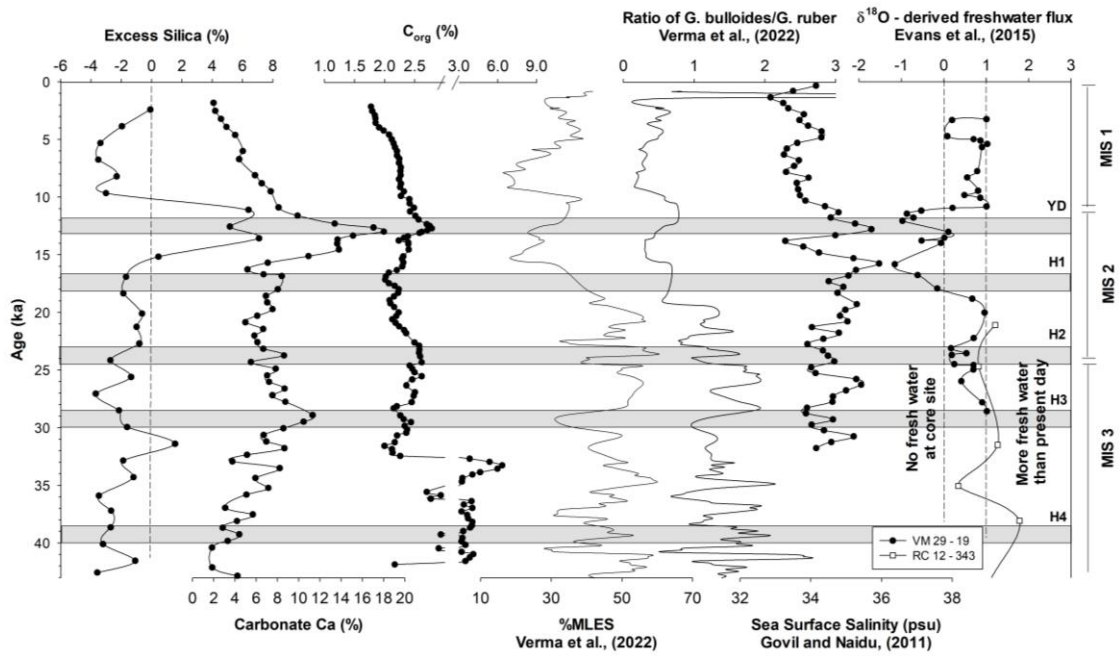
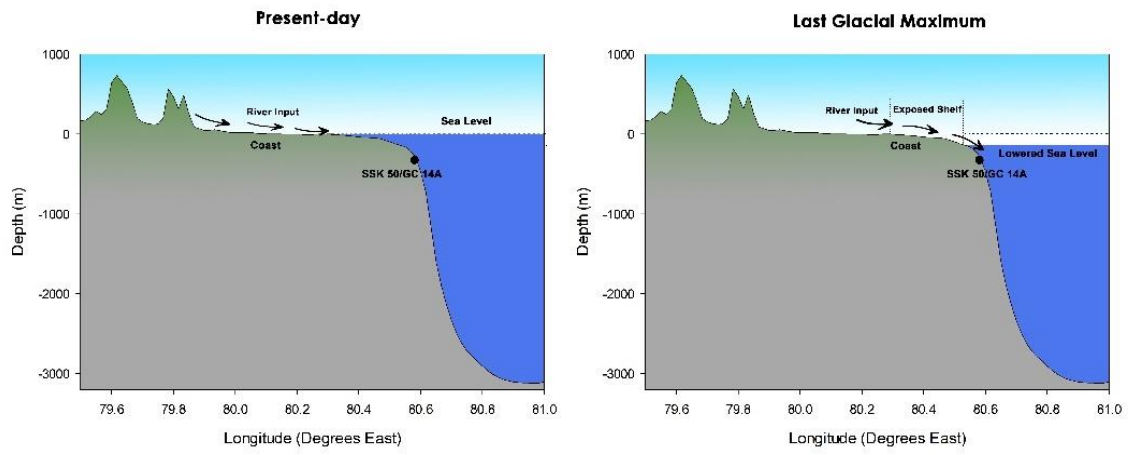


Figure 6



**Fig. 7**

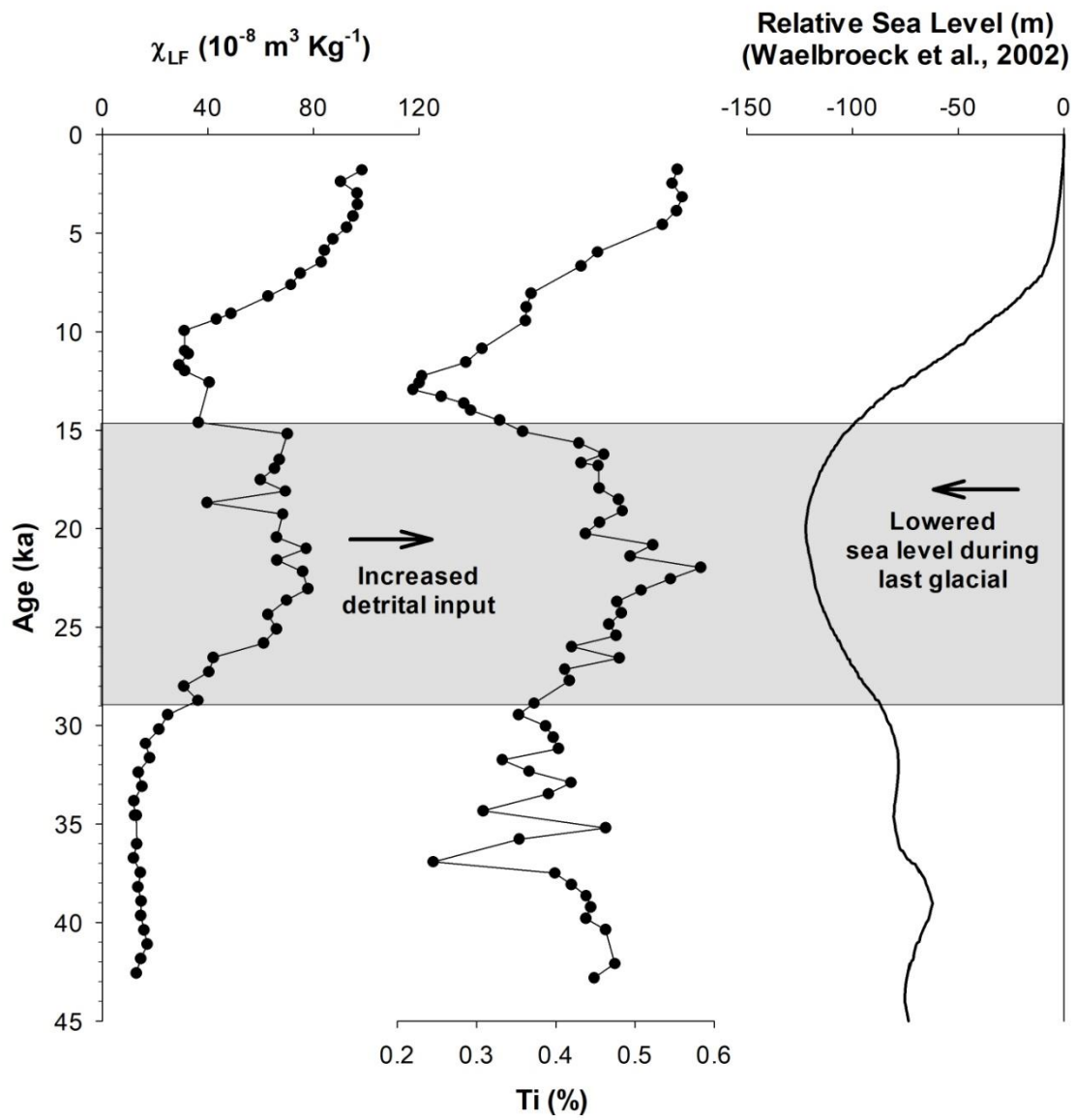


Figure 8

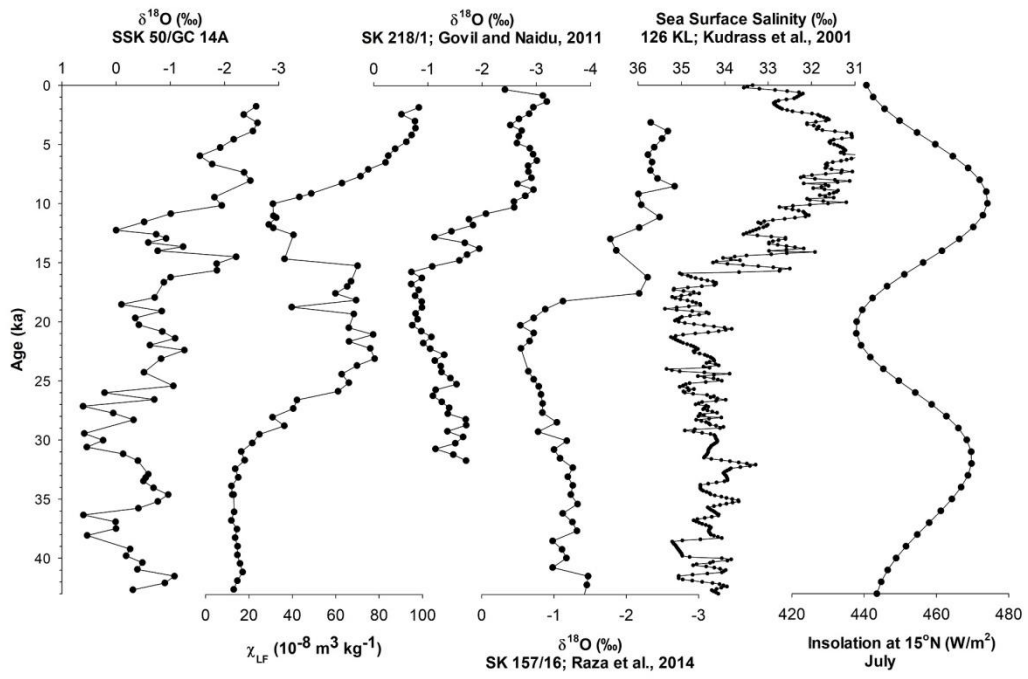


Figure 9



## Highlights

- An environmental magnetic and geochemical record of 42 kyr of detrital sedimentation from the western Bay of Bengal identified four periods of depositional change responding to monsoon
- Increased detrital input found at 24 – 15 ka due to subaerial erosion of exposed shelf during LGM sea-level low stand
- Weaker monsoon, weaker stratification and increased vertical mixing led to an enhanced biological productivity during 15–10 kyr BP
- Holocene period recorded increased chemical weathering in the source areas due to the monsoon intensification

# Graphical Abstract

